Effect of Anisotropic Thermal Conductivity on Deformation of a Thermoelastic Half-Space Subjected to Surface Loads

Kavita Rani*[1], Anil K. Vashishth[2], Kuldip Singh[3]
*[1]Department of Mathematics, CMG Govt. College for Women, Bhodia Khera, Fatehabad, Haryana, India
[2]Department of Mathematics, Kurukshetra University, Kurukshetra, Haryana, India
[3]Department of Mathematics, Guru Jambheshwar University of Science and Technology, Hisar , Haryana, India

ABSTRACT

The study is motivated by a desire to develop an analytical technique to study quasi-static plane strain deformation of a thermoelastic medium due to surface loads by taking into account the anisotropy of thermal conductivity. By applying the Laplace and Fourier transforms to the state variables involved in the basic governing equations, the solutions for the stresses, displacements, temperature difference and heat flux are obtained. Considering the boundary conditions, the problem is solved in the transformed domain. The actual solutions of the problem in the physical domain are acquired by inverting the Laplace-Fourier transform. Finally, some numerical examples are given to demonstrate the influences of the surface loads and the anisotropy of thermal conductivity on the thermo-elastic response.
Keywords: Anisotropy, Thermal conductivity, Surface loads, Thermoelastic.

I. INTRODUCTION

The thermo-elastic problems of the time-dependent behaviour of material with surface loads are significant and have received extensive attention in the field of geology, environmental engineering, soil science and civil engineering. The problems for thermal response and deformation caused by the thermal and mechanical loads have been studied by numerous investigators [1-12].

It is observed from practice that the typical deposit process of natural geomaterials may lead to clear differences in thermal conductivity between different directions, especially for the horizontal and vertical thermal conductivity. Therefore, some researchers focused their attention on the study of the thermo-elastic response of the material with anisotropic thermal conductivity. Pan [13] studied the transient thermoelastic deformation in a transversely isotropic and layered half-space by surface loads and internal sources. Wei and Yu-Qiu [14] discussed plane problem of orthotropic quasi-static thermoelasticity. Sharma and Kumar [15] investigated the plane strain problems in generalized theory of thermo-elasticity in a homogeneous transversely isotropic medium. Kögl and Gaul [16] presented a boundary element method for dynamic anisotropic coupled thermoelasticity and the results for quasi static and stationary thermoelasticity were also deduced. Youssef and El-Bary [17] discussed the thermal shock problem to the general case with variable thermal conductivity. Aouadi [18] studied the problem of variable electrical and thermal conductivity in the theory of generalised thermoelastic diffusion and discussed thermoelastic diffusion interactions in an infinitely long solid cylinder subjected to a thermal shock on its surface, which is in contact with a permeating substance.

Youssef and Abbas [19] used a finite element method to analyse transient phenomena in an infinitely long annular cylinder in the context of the theory of generalized thermoelasticity with one relaxation time considering the thermal conductivity to be variable. Ai *et al.* [20] derived an analytical solution for the axisymmetric thermo-elastic problem of multilayered material with anisotropic thermal diffusivity due to a buried heat source. Ai and Wang [21] discussed time dependent analysis of thermo-mechanical behaviour of a layered thermoelastic half-space with anisotropic thermal diffusivity. Ai and Wu [22] studied a thermal consolidation problem of a multilayered porous thermo-elastic medium with anisotropic thermal diffusivity and permeability due to a heat. Ezzat and El-Bary [23] used the theory of generalized magneto-thermoelasticity with variable thermal conductivity and fractional order of heat transfer and solved the problem of an infinite long hollow cylinder in the presence of an axial uniform magnetic field.

It is noted that although many problems involving thermal consolidation and thermomechanical response due to heat sources or thermal loading have been investigated, studies dealing with the quasi static plane strain deformation of a thermoelastic medium due to surface loads by taking into account the anisotropy of thermal conductivity are rather limited.

The objective of this paper is to introduce the analytical method to study the behaviour of thermoelastic material with anisotropic thermal diffusivity due to surface loads. The basic equations are governed by coupled theory thermoelasticity. The solutions in the Laplace– Fourier transformed domain are obtained by solving equations satisfying the boundary conditions. The actual solutions in the physical domain can be acquired by the inversion of the Laplace-Fourier transform. Finally, numerical examples are presented to investigate the effects of different material parameters on temperature difference, heat flux and variation of displacement.

The importance of the problem considered lies in the fact that the crust of the earth is anisotropic in different directions and therefore it is useful to study the effect of anisotropy on the static field due to surface loads.

II. FORMULATION OF THE PROBLEM

In this study, we consider the temperature distribution in a deformable body and therefore the corresponding model evokes the solution of a coupled thermomechanical problem. A homogeneous, thermoelastic half-space with anisotropic thermal conductivity is considered. The origin of a Cartesian coordinate system (x, y, z) is placed at the boundary of the half-space and the z -axis is drawn vertically into the medium.

Consider a strip $-L \le y \le L$ of infinite length on the surface of thermoelastic half-space. Let a normal load of force density σ_0 acting in positive direction of z be uniformly distributed over the strip (Fig1 a). For shear strip loading (Fig 1b), the force density is taken as τ_0 .

Since the source is long in one direction in comparison to others, two dimensional approximation is justified. So, a plane strain problem is studied in yz -plane and the displacement vector can be written as

$$\boldsymbol{u} = (u_y, u_z). \tag{1}$$

In case the material is homogeneous with anisotropic thermal conductivity, the heat flow obeys Fourier's law as

$$\boldsymbol{q} = -\nabla_\lambda \theta, \tag{2}$$

where $\boldsymbol{q} = (q_y, q_z)$ is heat flux vector; λ_y , λ_z are thermal conductivities in y and z directions respectively; $\nabla_\lambda \equiv \left(\lambda_y \partial_y, \lambda_z \partial_z \right)$ and θ is the temperature deviation from the reference temperature T_0 . $\partial_y(.)$ represents partial differentiation with respect to y .

By considering the coupling of elastic and thermal processes, the heat conduction equation with anisotropic thermal conductivity can be written as

$$(\nabla.\nabla_\lambda)\theta - \rho C_e\dot\theta - \beta T_0\dot e = 0, \qquad (3)$$

where, C_e is the specific heat, ρ is the density, $\beta = \alpha_t(3\lambda + 2\mu)$, λ and μ are Lame's constants, α_t is the coefficient of linear thermal expansion and $e = u_{y,y} + u_{z,z}$.

The Duhamel-Neumann relations establish the relationship between the state of stress, strain and temperature and can be written as

$$2\mu\varepsilon = C.\sigma + \alpha_0\theta I, \qquad (4)$$

where $\quad \sigma = \begin{bmatrix} \sigma_{yy} & \sigma_{yz} \\ \sigma_{yz} & \sigma_{zz} \end{bmatrix}$ and $\quad \varepsilon = \begin{bmatrix} \varepsilon_{yy} & \varepsilon_{yz} \\ \varepsilon_{yz} & \varepsilon_{zz} \end{bmatrix}$

$= \frac{1}{2}(\nabla u + \nabla^T u)$ are stress and strain tensors respectively, $\nabla \equiv (\partial_y, \partial_z)$, $\alpha_0 = 2\mu(1+\upsilon)\alpha_t$, $C = \begin{bmatrix} (1-\upsilon) & -\upsilon \\ -\upsilon & (1-\upsilon) \end{bmatrix}$, $I = \begin{bmatrix} 1 & 0 \\ 0 & 1 \end{bmatrix}$ and υ is Poisson's ratio.

The static equilibrium, with body force being neglected, is given by

$$\nabla.\sigma = 0, \qquad (5)$$

and the compatibility equation is

$$\varepsilon_{yy,zz} + \varepsilon_{zz,yy} = 2\varepsilon_{yz,yz}. \qquad (6)$$
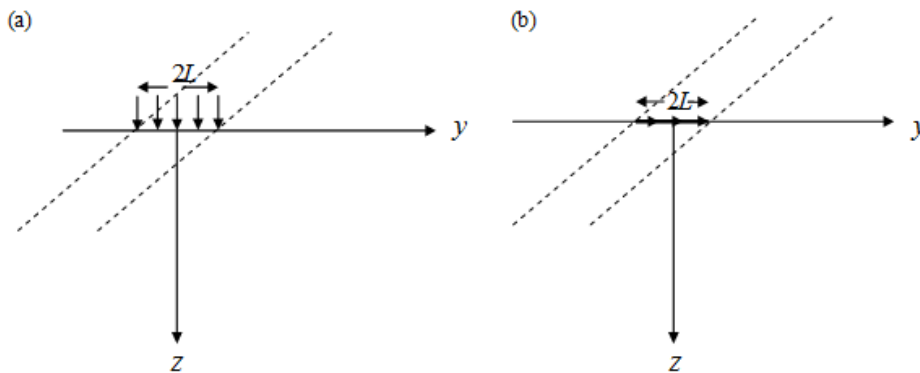
Figure 1. Geometry of the model (a) Normal strip load (b) Shear strip load

III. DERIVATION OF ANALYTICAL SOLUTION

The Airy stress function U is defined as

$$\sigma_{yy} = \partial_{zz}U, \quad \sigma_{zz} = \partial_{yy}U, \quad \sigma_{yz} = -\partial_{yz}U. \qquad (7)$$

Using Eqs. (4)-(5) and (7) in Eqs. (3) and (6), we get

$$\nabla^2(\nabla^2 U + 2\eta\theta) = 0, \qquad (8)$$

$$(\nabla.\nabla_\lambda)\theta - \left(\rho C_e + \frac{\alpha_0^2 T_0}{\mu(1-2\upsilon)}\right)\dot\theta - \frac{\alpha_0 T_0}{2\mu}(\nabla^2\dot U) = 0, \qquad (9)$$

where $\eta = \dfrac{\alpha_0}{2(1-\upsilon)}$, $\nabla^2 \equiv \nabla.\nabla$.

Taking Laplace transform of Eqs. (8) and (9), we obtain

$$(\nabla.\nabla_c - s)\nabla^2\theta = 0, \qquad (10)$$

$$(\nabla.\nabla_c - s)\nabla^4 U = 0, \qquad (11)$$

where, $c_i = \dfrac{\lambda_i(\lambda + 2\mu)}{\rho C_e(\lambda_s + 2\mu)}$, $\lambda_s = \lambda + \dfrac{T_0\beta^2}{\rho C_e}$,

$\nabla_c \equiv (c_y\partial_y, c_z\partial_z)$ and s is variable of Laplace transform.

Solving Eqs. (10) and (11), we have

$$\theta = \int_0^\infty R\binom{\sin ky}{\cos ky}dk, \quad U = \int_0^\infty F\binom{\sin ky}{\cos ky}dk, \qquad (12)$$

where $R = (A_1 e^{-mz} + A_2 e^{-kz})$,

$$F = (B_1 e^{-mz} + (B_2 + B_3 kz) e^{-kz}), \quad m = \left(\frac{c_y}{c_z} k^2 + \frac{s}{c_z} \right)^{1/2}$$

and A_i, B_i may be functions of k.

Making use of Eq. (12) in Eqs. (8)-(9), we get

$$A_1 = -\frac{s_a}{2\eta c_z} B_1, \quad B_3 = \frac{\alpha_0}{2k^2(v_s - v)} \left(1 + \frac{(s_a - s)(1 - v_s)}{s(1-v)} \right) A_2, \quad (13)$$

where $s_a = c_z(m^2 - k^2)$, $v_s = \dfrac{\lambda_s}{2(\lambda_s + \mu)}$.

Eq. (7) gives

$$\sigma_{zz} = \int_0^\infty N \binom{\sin ky}{\cos ky}(k)\,dk, \quad \sigma_{yz} = \int_0^\infty S \binom{\cos ky}{-\sin ky} k\,dk,$$

$$(14)$$

where $N = -k(B_1 e^{-mz} + (B_2 + B_3 kz) e^{-kz})$,

$S = (mB_1 e^{-mz} + ((B_2 - B_3)k + B_3 k^2 z) e^{-kz})$.

The displacement components can now be written as

$$2\mu u_y = \int_0^\infty V \binom{\cos ky}{-\sin ky}\,dk, \quad 2\mu u_z = \int_0^\infty W \binom{\sin ky}{\cos ky}\,dk,$$

$$(15)$$

where

$$V = -\left(B_1 e^{-mz} + (B_2 + B_3(2v - 2 + kz) + \frac{\alpha_0}{k^2} A_2) e^{-kz} \right) k,$$

$$W = (mB_1 e^{-mz} + (B_2 + B_3(1 - 2v + kz) - \frac{\alpha_0}{k^2} A_2) k e^{-kz})$$

IV. BOUNDARY CONDITIONS

For prescribed surface loads, assuming the surface to be non adiabatic isothermal, σ_{yz} and σ_{zz} are known at $z = 0$. So,

$$\sigma_{yz} = (\sigma_{yz})_0, \quad \sigma_{zz} = (\sigma_{zz})_0 \text{ and } \theta = 0 \text{ at } z = 0. \quad (16)$$

Let $(\sigma_{zz})_0 = \int_0^\infty N_0 \binom{\sin ky}{\cos ky} k\,dk$,

$$(\sigma_{yz})_0 = \int_0^\infty S_0 \binom{\cos ky}{-\sin ky} k\,dk. \quad (17)$$

Using Eqs. (16)-(17) in Eq. (14) and solving, we get

$$A_1 = -A_2 = -\frac{sk(v_s - v)(m+k)(S_0 + N_0)}{\eta\Omega},$$

$$B_1 = \frac{sk(v_s - v)(S_0 + N_0)}{(m-k)\Omega}, \quad B_2 = -B_1 - \frac{N_0}{k},$$

$$B_3 = \frac{(m+k)(S_0 + N_0)}{k\Omega} \left(s(v_s - v) + s_a(1 - v_s) \right), \quad (18)$$

where $\Omega = s(v_s - v)(k - m) - s_a(1 - v_s)(k + m)$.

Using these values of A_i and B_i's in equations (12), (14)-(15), the expressions for the temperature difference, stresses, displacements and heat flux are obtained. Values of S_0 and N_0 for different types of load are given in Table 1.

Table 1. Values of S_0, N_0 for different types of load on the surface.

	Normal strip loading	Normal line loading	shear strip loading	shear line loading
S_0	0	0	$-\dfrac{\tau_0}{\pi sk} \dfrac{\sin kL}{kL}$	$-\dfrac{\tau_0}{\pi sk}$
N_0	$-\dfrac{\sigma_0}{\pi ks} \dfrac{\sin kL}{kL}$	$-\dfrac{\sigma_0}{\pi ks}$	0	0
Upper solution/ Lower solution	Lower solution	Lower solution	Upper solution	Upper solution

V. SOLUTIONS FOR SURFACE LOADS

A. Normal Strip Loading

The expressions of displacements, stresses, temperature difference and heat flux solutions for normal strip loading are given by

$$2\mu u_y = -\frac{\sigma_0}{\pi s} \int_0^\infty [\frac{2sk(v_s - v)}{(m-k)} \left(e^{-mz} - e^{-kz} \right) - \{s(v_s - v)$$

$$+ s_a(1 - v_s)\} z(k+m) e^{-kz} + \frac{1}{k} \{s(v_s - v)(m-k)$$

$$- s_a(1 - 2v)(1 - v_s)(m+k)\} e^{-kz}] \frac{\sin kL}{kL} \frac{\sin ky}{\Omega}\,dk,$$

$$(19)$$

$$2\mu u_z = -\frac{\sigma_0}{\pi s} \int_0^\infty [\frac{2sm(v_s - v)}{(m-k)} \left(e^{-mz} - e^{-kz} \right) + \{s(v_s - v)$$

$$+ s_a(1 - v_s)\} z(k+m) e^{-kz}$$

$$+ \frac{2}{k} s_a(1 - v)(1 - v_s)(m+k) e^{-kz}] \frac{\sin kL}{kL} \frac{\cos ky}{\Omega}\,dk,$$

$$(20)$$

$$\sigma_{yz} = \frac{\sigma_0}{\pi s} \int_0^\infty [\frac{2sm(\upsilon_s - \upsilon)}{(m-k)}\left(e^{-mz} - e^{-kz}\right) + \{s(\upsilon_s - \upsilon)$$
$$+ s_a(1-\upsilon_s)\}z(k+m)e^{-kz}]\frac{\sin kL}{kL}\frac{\sin ky}{\Omega}kdk, \tag{21}$$

$$\sigma_{zz} = \frac{\sigma_0}{\pi s} \int_0^\infty [\frac{2sk(\upsilon_s - \upsilon)}{(m-k)}\left(ke^{-mz} - me^{-kz}\right) + \{s(\upsilon_s - \upsilon)$$
$$+ s_a(1-\upsilon_s)\}(1+kz)(k+m)e^{-kz}]\frac{\sin kL}{kL}\frac{\cos ky}{\Omega}dk, \tag{22}$$

$$\theta = \frac{\sigma_0(\upsilon_s - \upsilon)}{\pi\eta} \int_0^\infty (e^{-mz} - e^{-kz})(k+m)\frac{\sin kL}{kL}\frac{\cos ky}{\Omega}dk, \tag{23}$$

$$q_y = \frac{\sigma_0(\upsilon_s - \upsilon)\lambda_y}{\pi\eta} \int_0^\infty (e^{-mz} - e^{-kz})(k+m)\frac{\sin kL}{kL}\frac{\sin ky}{\Omega}dk, \tag{24}$$

$$q_z = \frac{\sigma_0(\upsilon_s - \upsilon)\lambda_z}{\pi\eta} \int_0^\infty (me^{-mz} - ke^{-kz})(k+m)\frac{\sin kL}{kL}\frac{\cos ky}{\Omega}dk. \tag{25}$$

B. Normal Line Loading

Taking the limit as $L \to 0$ with σ_0 fixed, the displacements, stresses, temperature difference and heat flux for normal line loading can be obtained. The expressions for the solutions can be obtained from equations (19)-(25) by removing the factor $\frac{\sin kL}{kL}$. Taking the limit $t \to \infty$, using the result that $\lim_{t\to\infty} f(t) = \lim_{s\to0} s\bar{f}(s)$, and evaluating the integrals given in Eqs. (19)-(25) analytically, we have $q_z = \theta = 0$ and the displacements and stresses obtained for this limiting case match with the corresponding solutions of elastic medium [24].

C. Shear Strip Loading

The solutions for shear strip loading are obtained as

$$2\mu u_y = \frac{\tau_0}{\pi s} \int_0^\infty [\frac{2sk(\upsilon_s - \upsilon)}{(m-k)}\left(e^{-mz} - e^{-kz}\right) + \{s(\upsilon_s - \upsilon)$$
$$+ s_a(1-\upsilon_s)\}z(k+m)e^{-kz}$$
$$- \frac{2}{k}\left(s_a(1-\upsilon)(1-\upsilon_s)(m+k)\right)e^{-kz}]\frac{\sin kL}{kL}\frac{\cos ky}{\Omega}dk, \tag{26}$$

$$2\mu u_z = -\frac{\tau_0}{\pi s} \int_0^\infty [\frac{2s(\upsilon_s - \upsilon)}{(m-k)}\left(me^{-mz} - ke^{-kz}\right) + \{s(\upsilon_s - \upsilon)$$
$$+ s_a(1-\upsilon_s)\}z(k+m)e^{-kz} - \frac{1}{k}\{s(\upsilon_s - \upsilon)$$
$$- s_a(1-2\upsilon)(1-\upsilon_s)(m+k)\}e^{-kz}]\frac{\sin kL}{kL}\frac{\sin ky}{\Omega}dk, \tag{27}$$

$$\sigma_{yz} = -\frac{\tau_0}{\pi s} \int_0^\infty [\frac{2s(\upsilon_s - \upsilon)}{(m-k)}\left(me^{-mz} - ke^{-kz}\right) + \{s(\upsilon_s - \upsilon)$$
$$+ s_a(1-\upsilon_s)\}(kz-1)(k+m)e^{-kz}]\frac{\sin kL}{kL}\frac{\cos ky}{\Omega}kdk, \tag{28}$$

$$\sigma_{zz} = \frac{\tau_0}{\pi s} \int_0^\infty [\frac{2sk(\upsilon_s - \upsilon)}{(m-k)}\left(e^{-mz} - e^{-kz}\right) + \{s(\upsilon_s - \upsilon)$$
$$+ s_a(1-\upsilon_s)\}z(k+m)e^{-kz}]\frac{\sin kL}{kL}\frac{\sin ky}{\Omega}dk, \tag{29}$$

$$\theta = \frac{\tau_0(\upsilon_s - \upsilon)}{\pi\eta s} \int_0^\infty (e^{-mz} - e^{-kz})(k+m)\frac{\sin kL}{kL}\frac{\sin ky}{\Omega}dk, \tag{30}$$

$$q_y = -\frac{\tau_0(\upsilon_s - \upsilon)\lambda_y}{\pi\eta s} \int_0^\infty (e^{-mz} - e^{-kz})(k+m)\frac{\sin kL}{kL}\frac{\cos ky}{\Omega}dk, \tag{31}$$

$$q_z = \frac{\tau_0(\upsilon_s - \upsilon)\lambda_z}{\pi\eta s} \int_0^\infty (me^{-mz} - ke^{-kz})(k+m)\frac{\sin kL}{kL}\frac{\sin ky}{\Omega}dk. \tag{32}$$

D. Shear line loading

As discussed earlier, the solutions for shear line loading can be obtained from equations (26)-(32 by removing the factor $\frac{\sin kL}{kL}$. For the limit $t \to \infty$, these results match with the corresponding results of elastic medium [24].

VI. NUMERICAL RESULTS AND DISCUSSION

It is seen that all the solutions are in Laplace-Fourier transformed domain. For computation of the inverse Laplace transform, Schapery's method [25] is used and the semi-infinite integral due to Fourier transform is computed numerically using Gauss quadrature formula.

As an example, we have computed the temperature difference, heat flux and components of displacement due to normal strip loading on the surface of a thermoelastic half-space with

anisotropic thermal conductivity. The parameters for thermoelastic medium are taken as

$$\mu = 7.1787 \times (10)^{10} kg\, m^{-1} s^{-2},$$
$$\lambda = 7.9663 \times (10)^{10} kg\, m^{-1} s^{-2},$$
$$\alpha_t = 3.35 \times (10)^{-5} K^{-1}, \rho = 3320 kg\, m^{-3}, \quad (33)$$
$$T_0 = 600K, C_e = 1055 m^2 K^{-1} s^{-2}.$$

To make the quantities dimensionless, the followings are defined

$$Y = \frac{y}{L}, Z = \frac{z}{L}, T = \frac{2c_z t}{L^2}, U_i = \frac{\mu u_i}{\sigma_0 L}, \Theta = \frac{\eta \theta}{\sigma_0},$$
$$\Sigma_{ij} = \frac{\sigma_{ij}}{\sigma_0}, Q_z = \frac{\eta L q_z}{\sigma_0 \lambda_z}, r = \frac{c_y}{c_z}. \quad (34)$$

Figure 2 shows the effect of anisotropy thermal conductivity on the variation of temperature difference with time at Y=0 due to normal strip loading. We notice that, near the source, anisotropy in thermal conductivity has only a small effect (Fig. 2a). As the depth increases, this effect becomes more significant (Fig. 2. b-d). At a given time, the temperature difference decreases as the thermal conductivity anisotropy parameter r increases. When the horizontal thermal conductivity is greater than the vertical thermal conductivity i.e. $r > 1$, at a given time; the temperature difference for an anisotropic isothermal half-space is less than the temperature difference for the corresponding isotropic isothermal half-space. As the depth increases, effect of r occurs delayed. In Fig. 2, curves for different values of the anisotropy parameter r coincide for very small and for very large times. This shows that the thermal conductivity anisotropy has no effect in the adiabatic and isothermal conditions.
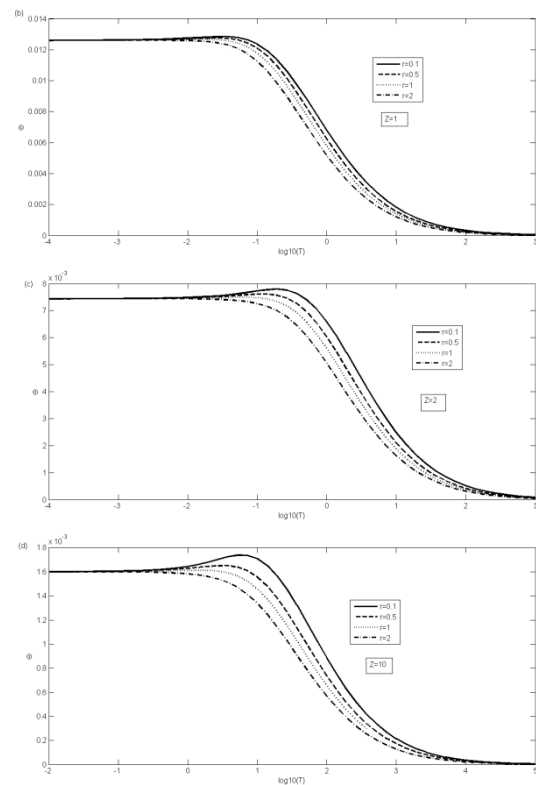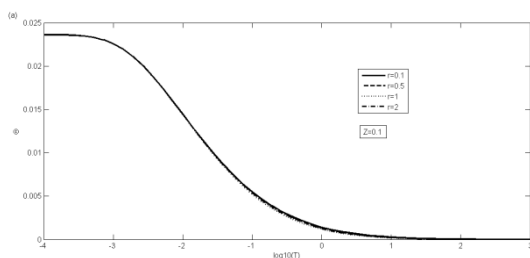
Figure 2. Effect of the value of anisotropic conductivity parameter r on temperature difference with time T for Y=0 and at depths (a) Z=0.1; (b) Z=1; (c) Z=2; (d) Z=10.

Figure 3 depicts the variation of the temperature difference with time at different depths for a small and large value of r. As the depth increases, temperature difference decreases along time and approaches to zero. For smaller Z, the variation is faster. Fig. 3 also indicates that the variation of temperature difference can reach its extremum value on the surface and becomes smaller and to be stable with the increase of time.

Figure 4 reveals the depth profile of the temperature difference at four times for small and large values of r. The temperature difference is zero at the surface, attains a maximum value at a depth depending upon r and T and then tends to zero as Z increases. Maximum value of Θ is shifted with time along Z.
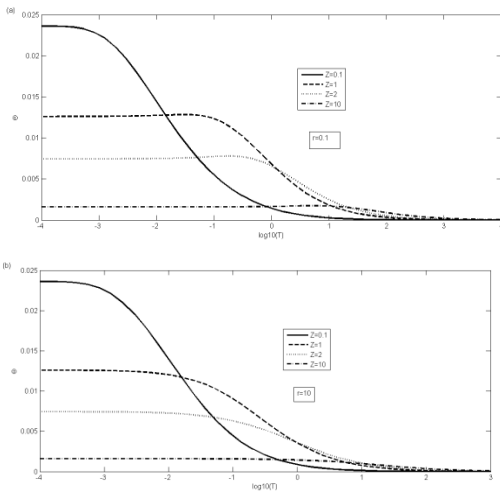
Figure 3. Variation of temperature difference with time T at four depths for (a) r=0.1, (b) r=10.
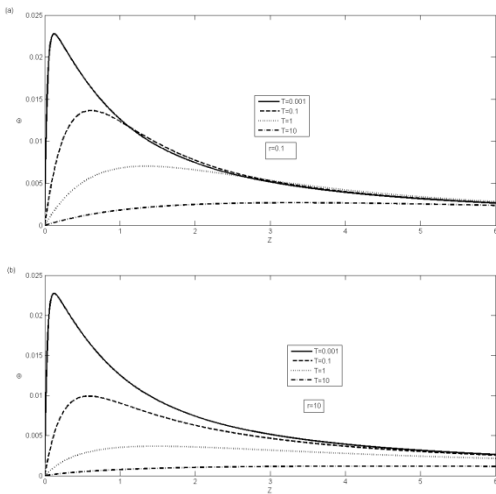
Figure 4. Depth profile of temperate difference at T=0.001, 0.1, 1, 10 for (a) r=0.1, (b) r=10.

Figure 5(a) shows the depth profile of the temperature difference for T = 0.001 for four values of r. Initially, a very large temperature difference develops near the surface resulting in a steep gradient of the temperature difference. No significant effect for different values of r is noticed. Figs 5(b)–(d) depict depth profile of Θ for T = 0.1, 1, 10. As T increases, the maximum value of the temperature difference decreases and the location of the maximum value travel down and shift right. The effect of increase of r is prominently increases with increase in T. Fig. 6 displays time history of the heat flux in the vertical direction at four depths (Z=0.1, 1, 2, 10) for r = 0.1, 10.

The heat flux pattern near the surface (Z=0.1) is significantly different from the patterns at depths. Figure 7 represents time history of the heat flux in vertical direction at different depths for four values of $r = 0.1, 1, 2, 10$.
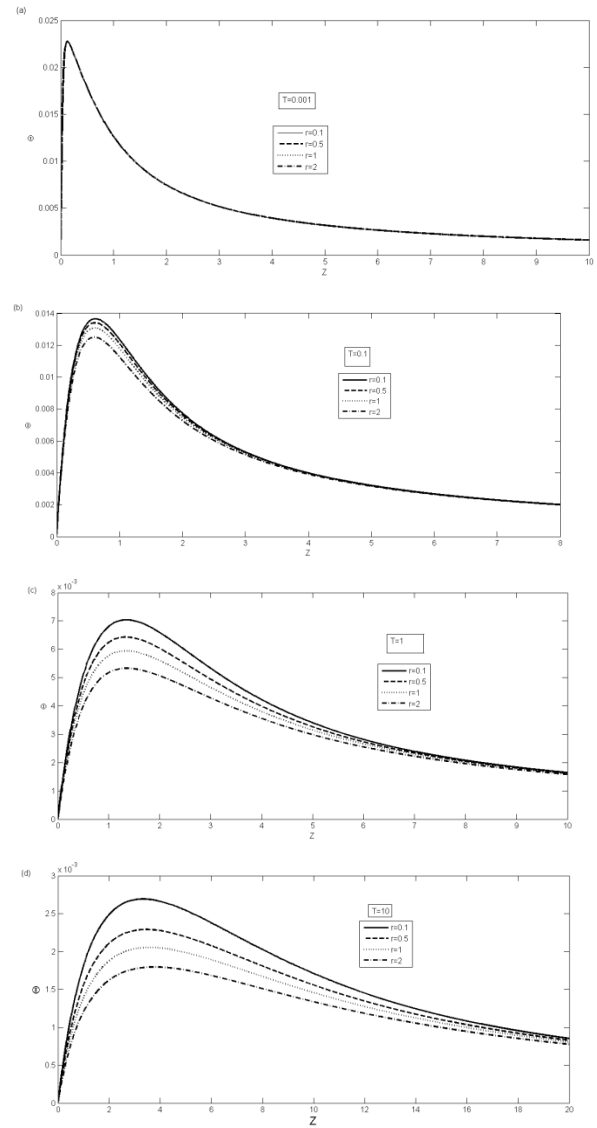
Figure 5. Effect of the value of anisotropic conductivity parameter r on temperature difference with depth for Y=0 and time (a) T=0.001; (b) T=0.1; (c) T=1; (d) T=10.
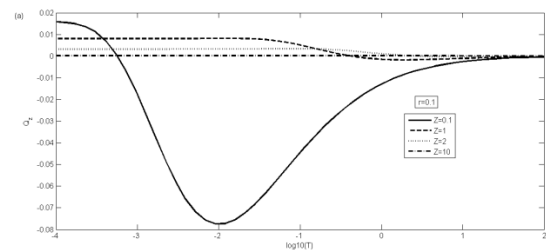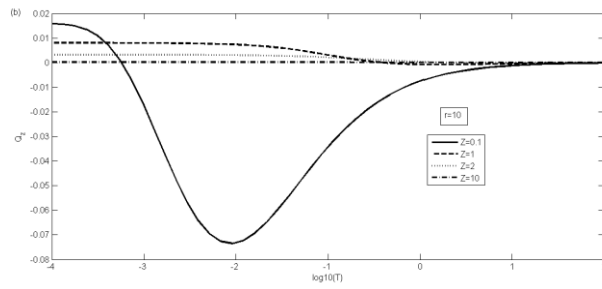
Figure 6. Variation of heat flux in vertical direction at four depths for (a) r=0.1, (b) r=10.
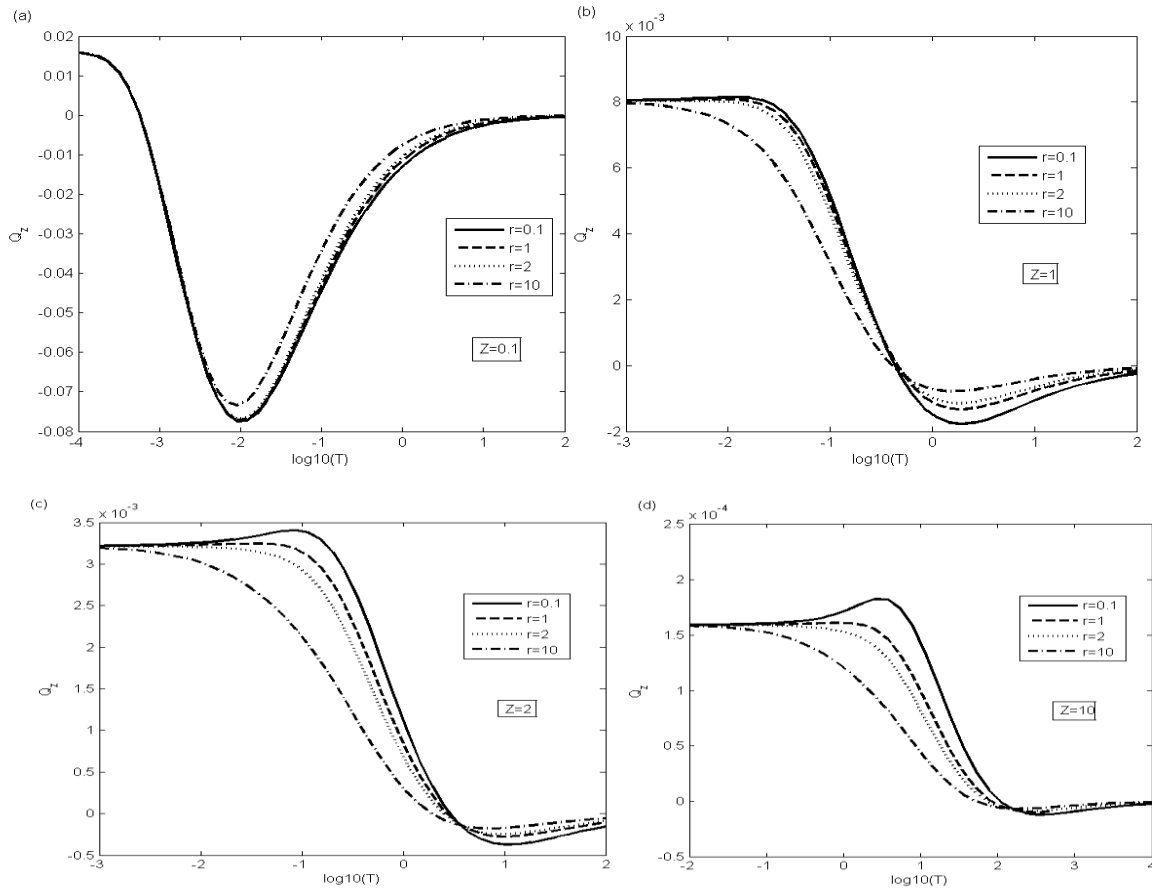
Figure 7. Effect of the value of anisotropic conductivity parameter *r* on temperature difference with time T at Y=0 and depths (a) Z=0.1; (b) Z=1; (c) Z=2; (d) Z=10.
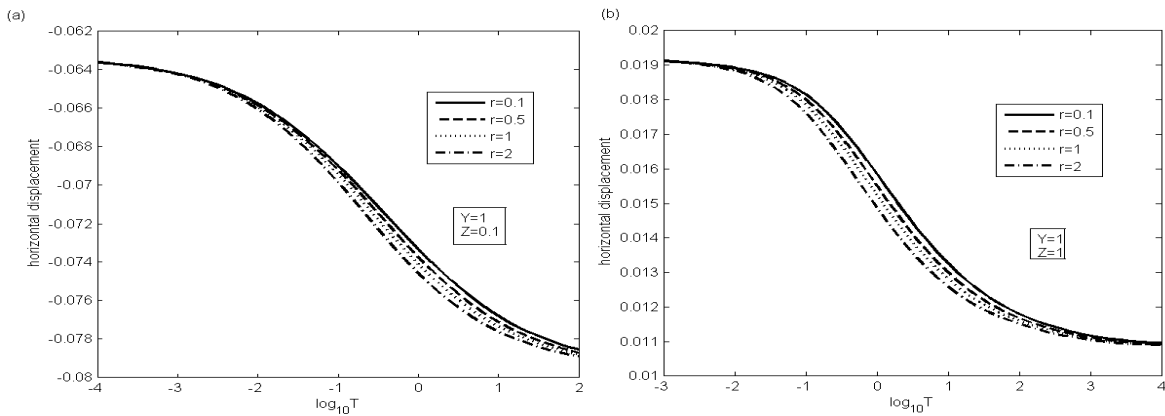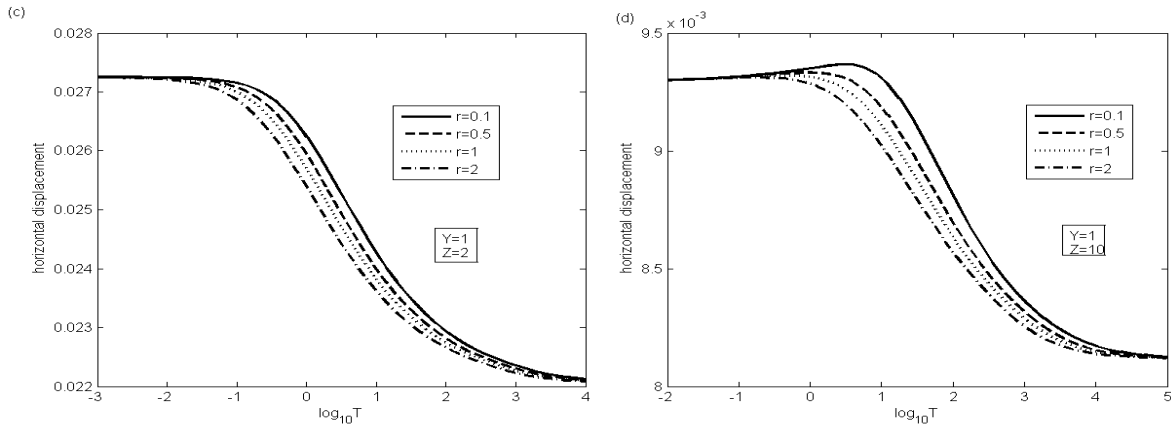
Figure 8. Effect of the value of anisotropic conductivity parameter r on horizontal displacement with time T for Y=0 and depths (a) Z=0.1; (b) Z=1; (c) Z=2; (d) Z=10.
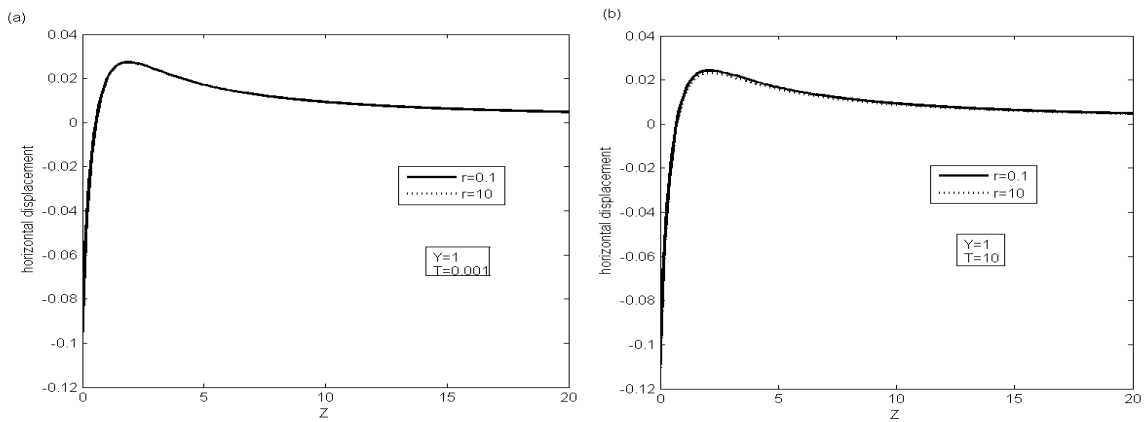
Figure 9. Depth profile of horizontal displacement at r =0.1, r =10 for (a) T=0.001, (b) T=10.
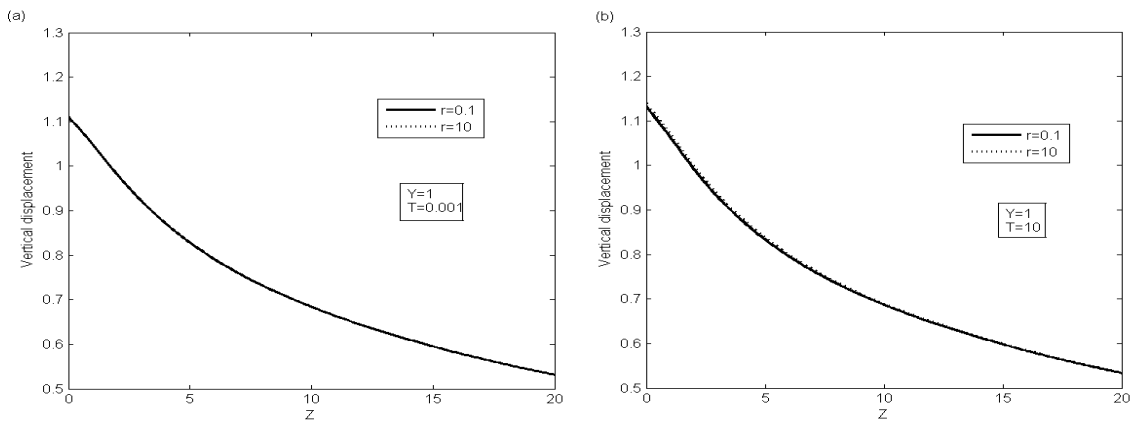
Figure 10. Depth profile of vertical displacement at r=0.1, r=10 for (a) T=0.001, (b) T=10.

990
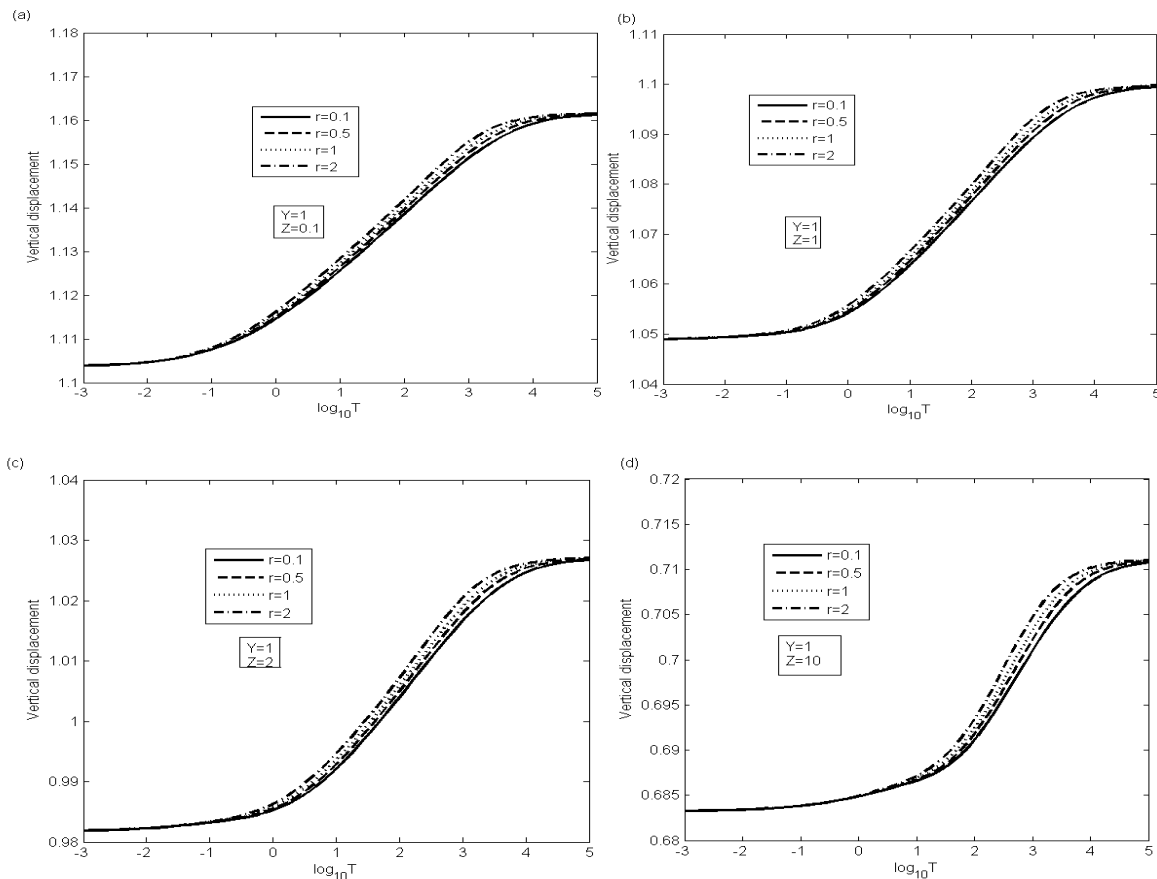
Figure 11. Effect of the value of anisotropic conductivity parameter r on vertical displacement with time T for Y=0 and depths (a) Z=0.1; (b) Z=1; (c) Z=2; (d) Z=10.

Time history of horizontal displacement at Y=1 for different depths $r = 0.1, 1, 2, 10$ is plotted in Figure 8. As the depth increases, horizontal displacement decreases along time and large value of r make it smaller. Depth profile of horizontal displacement at Y=1 is plotted in Figure 9 for two values of r. It increases quickly near the surface and then become stable and approaches to zero.

Variation of vertical displacement at Y=1 along Z is presented in Figure 10. It decreases with depth for all times. No significant effect of r seems on it. Time history of vertical displacement and effect of value of anisotropic thermal conductivity on it is shown in Fig 11 for four depths Z=0.1, 1, 2, 10 at Y=1. The vertical displacement increases with increase in time and increase in horizontal thermal conductivity. The curves for different values of r merge after a time. 7.

VII. CONCLUSION

In this paper, the quasi-static plane strain deformation of a thermoelastic half space with anisotropic thermal conductivity due to surface loads is studied. The problems of normal strip and line loading and shear strip and line loading are discussed in detail. Explicit analytical expressions in the Fourier-Laplace domain for the temperature function, heat flux, stresses and displacements have been obtained. From numerical computation, it is found that the anisotropy of thermal conductivity has a significant effect on deformation, temperature distribution as well as on heat transfer of the medium. However, the anisotropy has no effect for very small and large time (adiabatic and isothermal conditions).

991

VIII.   REFERENCES

[1]. Small J.C. and Booker J.R. 1984. Finite layer analysis of layered elastic materials using a flexibility approach. Part 1-Strip loadings. Int. J. Numer. Methods Eng., 20: 1025-1037.

[2]. Small J.C. and Booker J.R. 1986. Finite layer analysis of layered elastic materials using a flexibility approach. Part 2-circular and rectangular loadings. Int. J. Numer. Methods Eng., 23: 959-978.

[3]. Garg, N.R. and Singh, S. J. 1989. Quasi-static response of a layered half-space to surface loads. Indian J. Pure appl. Math, 20 (6): 621-631.

[4]. Garg, N. R., Singh, S.J. and Manchanda, S. 1991. Static deformation of an orthotropic multilayered elastic half -space by two dimensional surface loads. Proc. Indian Acad. Sci. (Earth Planet. Sci.), 100(2): 205-218.

[5]. Brock, L. M. and Rodgers, M. J. 1997. Steady state response of thermoelastic half-space to the rapid motion of surface thermal/mechanical loads. J. Elasticity, 47 (3): 225-240.

[6]. Brock, L.M., Georgiadis, H.G. and Tsamasphyros, G. 1997. The coupled thermoelasticity problem of the transient motion of a line heat/mechanical source over a half-space. J. Thermal Stresses, 20 (7): 773-795.

[7]. Sherief, H. H. and Megahed, A. F. 1999. A two-dimensional thermoelasticity problem for a half space subjected to heat sources. Int. J. Solids Struct., 36 (9): 1369-1382.

[8]. Kumar, R. and Deswal, S. 2001. Mechanical and thermal sources in a micropolar generalized thermoelastic medium. Journal of Sound and Vibration, 239 (3): 467-488.

[9]. Blond, E., Schmitt, N. and Hild, F. 2003. Response of saturated porous media to cyclic thermal loading. Int. J. Numerical Anal. Meth. Geomech., 27 (11): 883-904.

[10]. Furuya, M. 2005. Quasi-static thermoelastic deformation in an elastic half-space: Theory and application to InSAR observations at Izu-Oshima volcano, Japan. Geophys. J. Int., 161 (1): 230-242.

[11]. Shahani, A. R. and Nabavi, S.M. 2007. Analytical solution of the quasi-static thermoelasticity problem in a pressurized thick-walled cylinder subjected to transient thermal loading. Applied Mathematical Modelling, 31 (9): 1807-1818.

[12]. Lu, Z., Yao, H. and, Liu, G. 2010. Thermomechanical response of a poroelastic half-space soil medium subjected to time harmonic loads. Computers and Geotechnics, 37 (3): 343-350.

[13]. Pan, E. 1990. Thermoelastic deformation of a transversely isotropic and layered half-space by surface loads and internal sources. Physics of the Earth and Planetary Interiors, 60: 254-264.

[14]. Wei, L. and Yu-Qiu, Z. 1995. On the plane problem of orthotropic quasi-static thermoelasticity. J. Elasticity, 41 (3): 161-175.

[15]. Sharma, J. N. and Kumar, V. 1997. Plane strain problems of transversely isotropic thermoelastic media. J. Thermal Stresses, 20 (5): 463-476.

[16]. Kogl, M. and Gaul, L. 2003. A boundary element method for anisotropic coupled Thermoelasticity. Archive of Applied Mechanics, 73: 377-398.

[17]. Youssef, H.M. and El-Bary, A. A. 2006. Thermal shock problem of a generalized thermoelastic layered composite material with variable thermal conductivity. Math. Prob. Eng., 2006: 87940.

[18]. Aouadi M. 2006. A generalized thermoelastic diffusion problem for an infinitely long solid cylinder. Int J Math. Math. Sci., 2006: 25976.

[19]. Youssef, H. M. and Abbas, I. A. 2007. Thermal shock problem of generalized thermoelasticity for an infinitely long annular cylinder with variable thermal conductivity. Computational methods in Science and Technology, 13 (2): 95-100.

[20]. Ai, Z. Y., Wang, L. J. and Li, B. 2015. Analysis of axisymmetric thermo-elastic problem in multilayered material with anisotropic thermal diffusivity. Computers and Geotechnics, 65: 80-86.

[21]. Ai, Z. Y. and Wang, L. J. 2015. Time-dependent analysis of 3D thermo-mechanical behavior of a layered half-space with anisotropic thermal diffusivity. Acta Mech., 226 (9): 2939-2954.

[22]. Ai, Z.Y. and Wu, Q.L. 2016. The behavior of a multilayered porous thermo-elastic medium with anisotropic thermal diffusivity and permeability. Computers and Geotechnics, 76: 129-139.

[23]. Ezzat, M. A. and El-Bary, A. A. 2016. Effects of variable thermal conductivity and fractional order of heat transfer on a perfect conducting infinitely long hollow cylinder. International Journal of Thermal Sciences, 108: 62-69.

[24]. Sneddon, I.N. 1951. Fourier Transforms, McGraw-Hill, New York.

[25]. Schapery, R. A. 1962. Approximate methods of transform inversion for viscoelastic stress analysis. Proc. 4th US Nat. Congr. Appl. Mech., 2: 1075-1085.